Caveolin-1 is required for signaling and membrane targeting of EphB1 receptor tyrosine kinase

Meri M. Vihanto[1], Cecile Vindis[1,*], Valentin Djonov[2], Douglas P. Cerretti[3] and Uyen Huynh-Do[1,‡]

[1]Department of Nephrology and Hypertension, and Department of Clinical Research, Inselspital, University of Bern, CH-3010 Bern, Switzerland
[2]Institute of Anatomy, University of Bern, CH-3000 Bern, Switzerland
[3]Amgen Corporation, 1201 Amgen Court West, Seattle, WA 98101, USA

*Present address: Department of Biochemistry, INSERM U466, IFR-31, CHU Rangueil, 1, Avenue Jean Poulhès, TSA-50032, 31059 Toulouse Cedex 9, France
‡Author for correspondence (e-mail: uyen.huynh-do@insel.ch)

Accepted 17 February 2006
Journal of Cell Science 119, 2299-2309 Published by The Company of Biologists 2006
doi:10.1242/jcs.02946

Summary

Eph receptor tyrosine kinases are key players during the development of the embryonic vasculature; however, their role and regulation in adult angiogenesis remain to be defined. Caveolae are flask-shaped invaginations of the cell membrane; their major structural protein, caveolin-1, has been shown to regulate signaling molecules localized in these micro-domains. The interaction of caveolin-1 with several of these proteins is mediated by the binding of its scaffolding domain to a region containing hydrophobic amino acids within these proteins. The presence of such a motif within the EphB1 kinase domain prompted us to investigate the caveolar localization and regulation of EphB1 by caveolin-1. We report that EphB1 receptors are localized in caveolae, and directly interact with caveolin-1 upon ligand stimulation. This interaction, as well as EphB1-mediated activation of extracellular-signal-regulated kinase (ERK), was abrogated by overexpression of a caveolin-1 mutant lacking a functional scaffolding domain. Interaction between Ephs and caveolin-1 is not restricted to the B-subclass of receptors, since we show that EphA2 also interacts with caveolin-1. Furthermore, we demonstrate that the caveolin-binding motif within the kinase domain of EphB1 is primordial for its correct membrane targeting. Taken together, our findings establish caveolin-1 as an important regulator of downstream signaling and membrane targeting of EphB1.

Key words: Caveolae, Caveolin-1, Eph receptors, Ephrins, Signaling, Targeting

Introduction

Angiogenesis – the growth of novel capillaries from pre-existing vessels – is essential for several physiological processes such as embryonic development, wound healing, tissue regeneration and tissue remodeling (Folkman, 1995). However, under pathological conditions, uncontrolled angiogenesis sustains the progression of many diseases, including diabetic retinopathy, psoriasis, rheumatoid arthritis and tumor growth (Folkman, 1995). Signaling through receptor tyrosine kinases (RTKs) has a crucial role in these events. A subfamily of RTKs, the Eph receptors, is primarily expressed in endothelial cells from embryonic stages to adulthood (Gale and Yancopoulos, 1999), and they have emerged as essential regulators of angiogenesis in vivo, comparable in importance with vascular endothelial growth factor (VEGF) and angiopoietins. During the embryonic phase, Eph receptors regulate pivotal developmental changes including cell migration, axonal guidance and angiogenesis (Kullander and Klein, 2002). In the adult, they have been shown to be upregulated in several tumor tissues and presumably involved in pathogenic neovascularization. The mechanisms regulating their expression and functions, especially in the adult organism, remain to be defined.

Caveolae are flask-shaped invaginations of size 50-100 nm within the plasma membrane and are distinct from coated pits. They are found in most cell types, particularly in terminally differentiated cells such as adipocytes, muscle cells and endothelial cells. The putative functions of caveolae include cholesterol transport (Fielding and Fielding, 1995; Smart et al., 1996), endocytosis (Schnitzer et al., 1996) and signal transduction (Kurzchalia and Parton, 1999; Lisanti et al., 1994; Okamoto et al., 1998; Shaul and Anderson, 1998). They are rich in cholesterol, sphingomyelin and glycosphingolipids. The maintenance of cholesterol levels is essential for functional caveolae (Chang et al., 1992; Schnitzer et al., 1994) and depends, in part, on the interaction of cholesterol with caveolin-1, a major caveolae component (Smart et al., 1996). Recent insights into the physiological roles of caveolae and caveolins have been dissected in genetically modified mice (Drab et al., 2001; Razani et al., 2001). Caveolin-1 and caveolin-3 are dispensable during vascular and organ development but are essential for caveolae formation in specialized cells including most endothelia, adipocytes, and skeletal and cardiac myocytes. The ability of proteins to localize in caveolae, in addition to direct interactions of proteins with caveolins, has led to the hypothesis that caveolae might compartmentalize signaling in the plasma membrane and that the interactions (direct and indirect) between resident proteins and caveolin-1 might fine-tune the signaling cascades. In vitro data have shown that signaling molecules can potentially interact with caveolin-1, and that interactions with caveolin-1 can increase or decrease the fidelity or magnitude

of signaling (Engelman et al., 1998; Garcia-Cardena et al., 1996; Li et al., 1995). Caveolin-1 has a scaffolding domain, corresponding to amino acids 82-101, that can bind to a consensus sequence present in several signaling proteins, including epidermal growth factor (EGF) and platelet-derived growth factor (PDGF) receptors, the kinases Src and Fyn, and heterotrimeric G-proteins (Couet et al., 1997b; Li et al., 1995; Yamamoto et al., 1999). Two related caveolin-binding motifs (ϕxϕxxxxϕ and ϕxxxxϕxxϕ, where x is any amino acid and ϕ is one of the aromatic amino acids Trp, Phe or Tyr) have been identified, and these motifs exist within most caveolae-associated proteins (Couet et al., 1997a).

Incubation of endothelial cells with VEGF leads to a marked downregulation of both caveolae and caveolin-1 levels, whereas over-expression of caveolin-1 blocks VEGF-dependent activation of Elk-1 promoter activity (Liu et al., 1999). In addition, VEGF receptor-2 (VEGFR-2) is shown to localize in endothelial caveolae and associates with caveolin-1, and this complex is rapidly dissociated upon stimulation with VEGF, suggesting that caveolin-1 acts as a negative regulator of VEGFR-2 activity (Labrecque et al., 2003). By contrast, caveolin has also been shown to function as an activator of insulin receptor (IR) signaling (Yamamoto et al., 1998). In this work, we show that the EphB1 receptor signaling is initiated in low-density caveolar membrane domains and that caveolin-1 has an important role in this pathway. To define a more global significance of the caveolin-1 interaction with Eph receptors, we also show that an A-subclass Eph receptor, EphA2, interacts with caveolin-1. In addition, we demonstrate that the caveolin-binding motif in the kinase domain of EphB1 receptor is important for its membrane targeting. Our findings identify caveolae and caveolin-1 as important players in the regulation of EphB1 expression and signaling.

Results

A caveolin-binding motif is located within the kinase domain of EphB1 and EphA2 receptors

A putative caveolin-binding motif has been identified within the conserved kinase domain of many RTKs, including EGF receptor, insulin receptor, PDGF receptor, erbB2 and fibroblast growth factor receptor (FGF-R) (Couet et al., 1997a). We searched the cytoplasmic tail of the EphB1 and EphA2 receptors for this caveolin-binding motif, and identified a single caveolin-binding motif (ϕxϕxxxxϕ) within the kinase domain of EphB1 (WSYGVTVW; aromatic residues shown underlined) and EphA2 receptor (WSFGIVMW). We therefore hypothesized that caveolin-1 might have an important role in the regulation of Eph signaling.

EphB1 co-fractionates with caveolin-1 in CHO-EphB1 cells

We used the previously described (Vindis et al., 2003) and well-characterized CHO-EphB1 cells to examine the potential association of EphB1 receptor with caveolin-1 using an equilibrium sucrose density gradient centrifugation. This method has been commonly used to purify caveolar fractions from cultured cells (Li et al., 1996b; Song et al., 1996b) because these membrane subdomains contain high levels of cholesterol and sphingolipids with characteristic low buoyant density (Brown and London, 1998). A carbonate-based fractionation scheme was employed for the purification of caveolin-enriched membranes. Under these gradient conditions, caveolin-1 migrated in the low-density region (fractions 1-3) of the sucrose gradient consistent with lipid raft enrichment. Fig. 1A shows that EphB1 receptors were similarly distributed and co-fractionated with caveolin-1 in CHO-EphB1 cells. We used Src to show localization of a cytoplasmic protein, a significant fraction of which is expressed outside caveolae domains (fractions 6-8). Although, under certain experimental settings, Src has been shown to co-fractionate with caveolae-associated proteins (Song et al., 1996a), this is only a sub-fraction of its cellular expression. Src has also been detected in the cytoplasm and in the perinuclear Golgi region of the cell (Resh and Erikson, 1985; Willingham et al., 1979). In particular, 30-40% of the total Src population is localized to the perinuclear region of the cell (Tanaka and Kurth, 1984; Resh and Erikson, 1985). In our experiments, the majority of the Src protein localized outside the caveolae domains. This is in agreement with previous work from Prinetti et al., who showed that, in rat cerebellar granule cells, high-density membrane fractions of the sucrose gradient were enriched in Src and other Src-family protein tyrosine kinases (Prinetti et al., 2001).

EphB1 and EphA2 interact with caveolin-1 in response to ligand stimulation

The association of EphB1 receptor with caveolin-1-rich, low-density membrane fractions provided the first evidence that this receptor possibly interacts with caveolin-1. However, the co-localized subcellular distribution does not indicate a direct interaction between the two molecules. To evaluate further the potential interaction of EphB1 receptor with caveolin-1, we used two independent approaches: co-immunoprecipitation and immunofluorescence analyses. Fig. 1B shows that EphB1 receptor co-immunoprecipitates with caveolin-1 only when receptor is stimulated with ephrinB2 ligand in CHO-EphB1 cells. This direct interaction was time dependent, being most prominent between 30 and 60 minutes of stimulation. Caveolin-1 expression was stable during the time course and served as a loading control for the co-immunoprecipitation. One concern is that interaction between EphB1 and caveolin-1 could be an artefact, since the ephrinB2/Fc fusion proteins bound to EphB1 might also bind to the protein A-agarose. Two arguments speak clearly against this. First, the time-course of the interaction shows an increase followed by a decrease in the amount of bound EphB1 (maximal after 30 minutes of ligand stimulation, then much weaker EphB1-caveolin-1 interaction after 90 minutes). Second, when we used non-specific rabbit IgG, we were not able to co-immunoprecipitate any Eph receptor, especially after 30 minutes of ligand stimulation (a time point corresponding to the peak mentioned above) (Fig. 1B,D).

Next we used double immunofluorescence microscopy to examine the global co-localization of the EphB1 receptor with caveolin-1 in the plasma membrane. EphB1 receptor co-localized with caveolin-1 after 30 minutes of ligand stimulation, as demonstrated by the yellow areas in the superimposed images (Fig. 1C2). No co-localization was seen when the EphB1 receptors were left unstimulated (Fig. 1C1).

The caveolin-binding motif was not unique to EphB1, since we were able to identify it in all Eph receptors of both A and B subclasses. Therefore, to define a more global significance

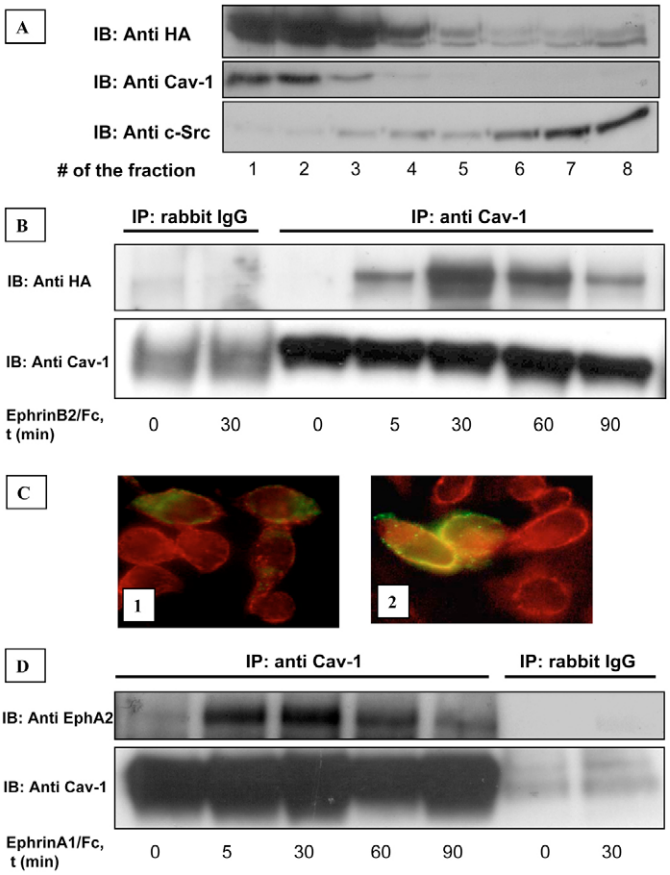

Fig. 1. Ligand-stimulated Eph receptors interact with caveolin-1. (A) Co-fractionation of EphB1 receptor with caveolin-1. Sucrose gradient centrifugations were performed as described previously (Song et al., 1996a). Fractions were collected and subjected to immunoblotting (IB) with antibodies directed against HA-tagged EphB1 receptor (Anti HA) and caveolin-1 (Anti Cav-1). EphB1 receptor and caveolin-1 located to the same, buoyant membrane fractions (#1-3). Immunoblotting with antibodies directed against Src (Anti c-Src) was used to show localization of a cytoplasmic protein, as it was located to the high-density fractions (#6-8). (B) Co-immunoprecipitation (IP) of EphB1 receptor with antibody against caveolin-1 in CHO-EphB1 cells. EphrinB2/Fc was added to the cells for indicated times, then cells were lysed, caveolin-1 (lanes 3-7) and control rabbit IgG (lanes 1-2) immunoprecipitates were resolved by SDS-PAGE and transblotted to PVDF membranes. Membranes were reciprocally immunoblotted with antibodies against HA or caveolin-1, respectively. (C) Immunofluorescence analysis confirmed the association of EphB1 receptor with caveolin-1 on the plasma membrane after 30 minutes of ephrinB2 ligand stimulation (C2) compared with non-stimulated cells (C1). CHO-EphB1 cells were fixed and stained with primary antibodies against HA and caveolin-1 followed by Alexa green- and red-conjugated secondary antibodies, respectively. Samples were processed as described under Materials and Methods. Images were acquired with a Nikon Eclipse E600 microscope, connected to Nikon digital camera DXM1200, and processed with the Nikon AC-1 software version 2.11. Magnification, ×1000. (D) Co-immunoprecipitation of EphA2 receptor with antibody against caveolin-1 in PC-3 cells. EphrinA1/Fc was added to the cells for indicated times, then cells were lysed, caveolin-1 (lanes 1-5) and control rabbit IgG (lanes 6-7) immunoprecipitates were resolved by SDS-PAGE and transblotted to PVDF membranes. Membranes were reciprocally immunoblotted with antibodies against EphA2 or caveolin-1, respectively. Results are representative of at least three independent experiments.

of the caveolin-1 interaction with Ephs, we studied the association of an A-subclass Eph receptor with caveolin-1. In previous work (Vihanto et al., 2005), we showed that PC-3 cells express high endogenous levels of EphA2. When we stimulated these cells with ephrinA1/Fc, we found a strong association between EphA2 and caveolin-1. Fig. 1D shows that this direct interaction was time dependent, being most prominent after 30 minutes of stimulation. Caveolin-1 expression was stable during the time course and served as a loading control for the co-immunoprecipitation.

EphrinB2 stimulates the phosphorylation of caveolin-1 on Tyr14

It has previously been shown that insulin stimulates the tyrosine phosphorylation of caveolin-1 by insulin receptor (Kimura et al., 2002). Similarly, we observed that ephrinB2 activated caveolin-1 phosphorylation in CHO-EphB1 cells in a time-dependent manner using a phosphospecific antibody recognizing phosphorylated Tyr14 of caveolin-1 (Fig. 2A) and we confirmed the results with immunofluorescence analysis using the same antibody (Fig. 2B). By contrast, in CHO cells without stably transfected EphB1 receptors, tyrosine phosphorylation of caveolin-1 was not stimulated when the ephrinB2 ligand was added (Fig. 2C).

Cholesterol depletion inhibits activation of the ERK/MAPK pathway by EphB1

We then examined the effects of cholesterol depletion on caveolae structure in relation to Eph signaling. It has previously been shown that, following treatment with 10 mM β-cyclodextrin (β-CD), caveolae invaginations almost vanish and may be discerned as minor irregular structures at the membrane surface (Parpal et al., 2001). We confirmed this observation by using transmission and scanning electron microscopy analyses, which clearly showed that the 10 mM β-CD treatment abolished almost all of the caveolae invaginations from the cell surface of CHO-EphB1 cells when compared with untreated cells (Fig. 3A). The β-CD-induced depletion of cholesterol from the CHO-EphB1 cells did not affect the ability of EphB1 receptor to co-immunoprecipitate with caveolin-1 (Fig. 3B). However, cholesterol depletion resulted in approximately 50% reduction in the relative phosphorylation levels of ERK/MAPK activation by EphB1 (Fig. 3C). These findings are in agreement with previous studies showing that cholesterol depletion inhibits ERK activation either by VEGF in bovine aortic endothelial cells (BAECs) (Labrecque et al., 2003) or by endothelin-1 in rat portal veins (Zeidan et al., 2003).

EphB1 mutants lacking the caveolin-binding motif fail to localize to the cell membrane

Previous studies have demonstrated that aromatic residues within the caveolin-binding motif of several proteins are essential for interaction with caveolin-1 (Couet et al., 1997a). Therefore, we designed several EphB1 receptor mutants by site-directed mutagenesis to disrupt the binding motif present in the kinase domain of the receptor, and to evaluate their impact on EphB1 receptor function. In the W815F mutant, the

distal aromatic amino acid in the binding motif was changed to phenylalanine. The W808A and Y810A mutants disrupt the binding motif at the proximal and central aromatic residues, respectively. A triple mutation (W808A/Y810A/W815F) replaces all three aromatic amino acids with alanine or phenylalanine. CHO cells transfected with the wild-type receptor expressed a high level of EphB1 receptor both at mRNA and protein levels (Fig. 4A,B). However, in agreement with results obtained from insulin receptor mutants lacking a correct caveolin-binding motif (Nystrom et al., 1999), cell-surface expression of the caveolin-binding motif mutants was strongly reduced, although the mRNA expression of the mutants was well detected (Fig. 4A,B).

To visualize the receptors at the cell membrane, we expressed HA-tagged wild-type or caveolin-binding-motif mutant EphB1 receptors in CHO cells and detected membrane localization by confocal microscopy. As seen in Fig. 5, mutant EphB1 receptors in which 1 or 3 of the aromatic residues were changed to alanine or phenylalanine were less expressed and failed to translocate to the plasma membrane, whereas the wild-type receptor clearly localized to the cell membrane. We also examined the co-localization of wild-type or mutant EphB1 receptors at the plasma membrane with caveolin-1. Caveolin-1 was abundantly expressed and clearly visualized at the membrane in all of the experiments (Fig. 5). Co-localization of wild-type EphB1 receptor with caveolin-1 was only seen in CHO cells transfected with wild-type EphB1 receptor or in CHO-EphB1 cells (Fig. 5C,D and 5O,P respectively), whereas all the mutants did not show any co-localization with caveolin-1 (Fig. 5E-N). Thus, our results provide evidence that the caveolin-binding motif is important for the membrane targeting of EphB1 receptors.

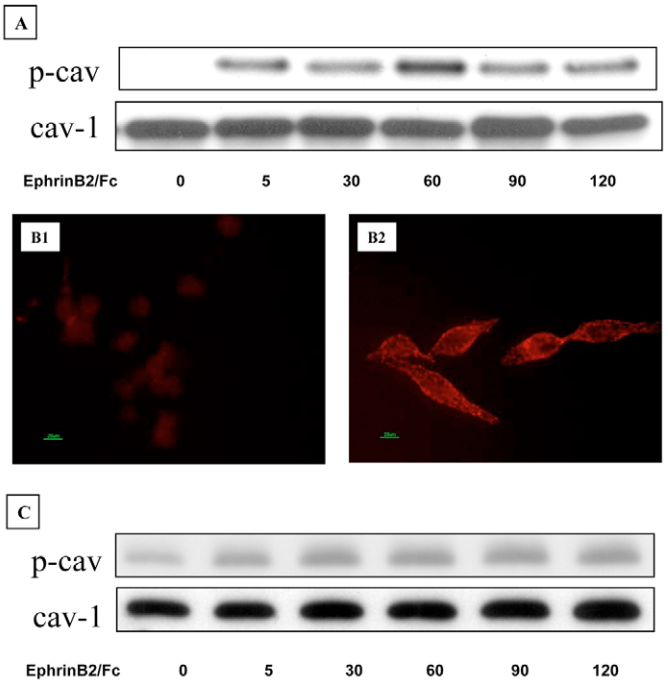

Fig. 2. EphrinB2 stimulates tyrosine phosphorylation of caveolin-1 at Tyr14. (A) CHO-EphB1 cells were serum starved for at least 24 hours, then stimulated for indicated times with 1-2 μg/ml ephrinB2/Fc. Cell lysates were separated by SDS-PAGE, transferred to PVDF membranes, and blotted with antibodies against phospho-caveolin (p-cav, upper panel) or caveolin-1 (cav-1, lower panel). (B) Immunofluorescence analysis confirmed the increasing tyrosine phosphorylation of caveolin-1 up to 60 minutes after ephrinB2 ligand stimulation (B2) compared with non-stimulated cells (B1). Thereafter, the phosphorylation of caveolin-1 decreased steadily. CHO-EphB1 cells were fixed and stained with primary antibody against phospho-caveolin followed by Alexa red-conjugated secondary antibody. Samples were processed as described under Materials and Methods. Images were acquired with a Nikon Eclipse E600 microscope, connected to Nikon digital camera DXM1200, and processed with the Nikon AC-1 software version 2.11. Bars, 20 μm. (C) CHO cells were serum starved for at least 24 hours, then stimulated for indicated times with 1-2 μg/ml ephrinB2/Fc. Cell lysates were separated by SDS-PAGE, transferred to PVDF membranes, and blotted with antibodies against phospho-caveolin (upper panel) or caveolin-1 (lower panel). Results are representative of at least three independent experiments.

The caveolin-1 scaffolding domain is required for EphB1-caveolin interaction and ERK activation by EphB1

To define the role of caveolin-1 on EphB1 signaling, we chose to use Cos-7 cells lacking endogenous caveolin-1 (Nystrom et al., 1999) to assess clearly the effect of reconstitution by wild-type or mutant caveolin-1. By immunoblotting and immunofluorescence analyses, we confirmed that Cos-7 cells express almost no endogenous caveolin-1 when compared with Cos-7 cells transiently transfected with caveolin-1 or when compared with CHO-EphB1 cells (Fig. 6A,B). Under our experimental conditions, transfection efficiencies were approximately 70% as determined by expression of green fluorescent protein (data not shown). Myc-tagged wild-type caveolin-1 (Cav-wt) was expressed at levels comparable with mutant caveolin-1 (Cav-mut) containing F92A and V94A point mutations in the scaffolding domain of caveolin-1 (Fig. 6C, lower panel).

Next, we performed co-immunoprecipitation experiments in Cos-7 cells transiently expressed with Cav-wt or Cav-mut and additionally with wild-type EphB1 receptor (Fig. 6C). Cav-wt co-immunoprecipitated with EphB1 receptors only after ligand stimulation; however, the point mutations in Cav-mut completely abolished the ability of caveolin-1 to interact with EphB1 (Fig. 6C, upper panel), a finding similar to studies with the insulin receptor (Nystrom et al., 1999). In addition, we showed that the phosphorylation of ERK is completely abolished in cells transfected with Cav-mut (Fig. 6C, lower panel).

Finally, to confirm the role of the caveolin-binding motif of EphB1 by an independent method, we performed immunofluorescence analysis of Cos-7 cells transiently transfected with Cav-wt or Cav-mut constructs and additionally with wild-type or mutant EphB1 receptor. Fig. 6D2 shows that only wild-type receptor co-localizes to the cell membrane with Cav-wt. Mutant EphB1 receptor shows no plasma membrane localization (Fig. 6D3,5), whereas both Cav-wt and Cav-mut localized on the cell surface (Fig. 6D2,3 and 6D4,5, respectively). Together, our results demonstrate that association of EphB1 with caveolin-1, as well as EphB1-induced ERK activation, is strongly dependent upon the caveolin-1 scaffolding domain, whereas targeting of EphB1 to the cell membrane requires an intact caveolin-1-binding motif.

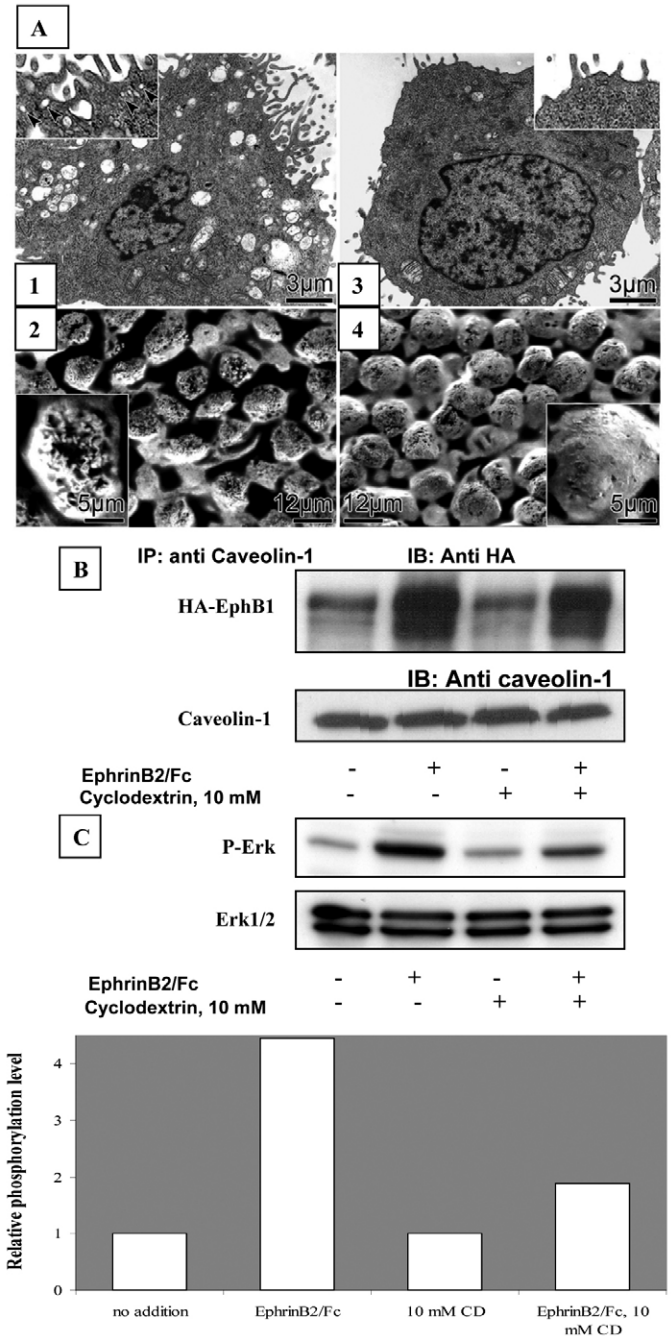

Fig. 3. Cholesterol depletion inhibits activation of the ERK/MAPK pathway by EphB1. (A) CHO-EphB1 cells were incubated with 0 (Fig. A1,2) or 10 mM (Fig. A3,4) β-cyclodextrin (β-CD) for 60 minutes, when cells were prepared for electron microscopy as described under Materials and Methods. Transmission electron microscopy (Fig. A, panels 1 and 3) and scanning electron microscopy (Fig. A, panels 2 and 4) reveal caveolae structures on the surface of the untreated CHO-EphB1 cells, indicated by arrowheads (insert in Fig. A1). Bars, 3 μm (panels 1,3), 12 μm (panels 2,4), and 5 μm (inserts in panels 2,4). A single cell is shown in the inserts shown in panels 2 and 4. (B,C) CHO-EphB1 cells were incubated with or without 10 mM β-CD for 60 minutes, and then stimulated with 1-2 μg/ml ephrinB2 ligand for 30 minutes. (B) Co-immunoprecipitation (IP) of EphB1 receptor with antibody against caveolin-1 in CHO-EphB1 cells. The immunoprecipitates were resolved by SDS-PAGE and transblotted to PVDF membranes. Membranes were reciprocally immunoblotted with antibodies against HA or caveolin-1, respectively. (C) The state of ERK phosphorylation was determined by immunoblotting with a phosphospecific antibody against active ERK (P-Erk). Stripped membranes were then reblotted with antibody against ERK (Erk1/2). Relative phosphorylation levels are given as a ratio of phosphorylated protein expression to unphosphorylated protein expression. Protein expressions were analyzed using Image J software (http://rsb.info.nih.gov/ij/). Results are representative of at least three independent experiments.

Discussion

The targeting of Eph receptor activity as a means of blocking angiogenesis and tumor growth has received considerable attention in recent years (Brantley et al., 2002; Dobrzanski et al., 2004; Mao et al., 2004). However, there are still considerable gaps in our knowledge of the mechanisms involved in the regulation of Eph receptor function and expression, and its relationship to angiogenic properties.

In recent years, caveolin-1 has emerged as an important regulatory molecule in signal transduction. Part of the controversy about the pro- and anti-angiogenic effects of caveolin could also arise from the multiple, and sometimes opposite, roles played by caveolin and caveolae. Indeed, whereas caveolin is known to repress the catalytic activity of various enzymes, caveolae are thought to facilitate and amplify signaling cascades through the compartmentalization of receptors with their effectors and mediators (Razani et al., 2002; van Deurs et al., 2003), a process named 'the caveolar paradox' (Feron and Kelly, 2001). These considerations, along with our observation that both A- and B-subclass Eph receptors – EphA2 and EphB1, respectively – contain a caveolin-binding motif, led us to investigate the localization and regulation of EphB1 receptor activity in caveolae structures. Indeed, we found that caveolae membrane domains are highly enriched in both EphB1 receptors and caveolin-1 in CHO-EphB1 cells. Such compartmentalization has been shown to be crucial for several signaling pathways, such as those triggered by EGF (Mineo et al., 1996) and PDGF (Liu et al., 1996), possibly allowing efficient interactions between key signaling proteins that are required for both positive and negative regulation of these activities.

One important observation of this study is that, under resting conditions, caveolin-1 is dissociated from the inactive form of EphB1 receptor and undergoes rapid association with the receptor upon stimulation with ephrinB2. This is also true for an A-subclass Eph receptor, EphA2, which associated with caveolin-1 only upon ephrinA1 stimulation. This provided us with further evidence that caveolin-1 functions as a global regulator of Eph signaling in different cell lines. In addition, stimulation of CHO-EphB1 cells with ephrinB2/Fc resulted in a marked increase in the tyrosine phosphorylation of caveolin-1 at Tyr14, which has been recognized as the principal residue phosphorylated by Src kinases (Li et al., 1996a). To prove that the enhanced tyrosine phosphorylation of caveolin-1 was indeed dependent on the activated EphB1 receptor, we repeated the experiment with CHO cells, which showed no significant increase in the tyrosine phosphorylation of caveolin-1. Previously, it has been shown that caveolin-1 is phosphorylated in response to growth factors such as EGF and insulin (Kim et

al., 2000; Kimura et al., 2002). However, caveolin-1 phosphorylation seems to be cell-type specific and stimulus specific because it was not observed in adrenal cortex endothelial cells after VEGF stimulation (Esser et al., 1998) or in BAECs under shear stress condition (Fujioka et al., 2000). Insulin stimulates tyrosine phosphorylation of caveolin-1 only in fully differentiated 3T3-L1 adipocytes but not in pre-adipocytes, although both cell types express caveolin and active insulin receptors (Mastick and Saltiel, 1997). The functional consequences of caveolin tyrosine phosphorylation are not yet fully understood. It has been postulated that the tyrosine phosphorylation of caveolin-1 at residue 14 could confer binding to SH2-domain-containing proteins and subsequent growth-stimulatory or oncogenic activity (Lee et al., 2000).

β-CD is a widely used tool to extract cholesterol from the plasma membrane of intact cells. Without itself incorporating into the membrane, β-CD selectively extracts cholesterol from the surface of the cells (Christian et al., 1997; Yancey et al., 1996). Using transmission and scanning electron microscopy analyses, we identified caveolae structures on the membrane of the untreated cells. They are characterized by frequent round structures of ~50 nm in diameter. We demonstrated that 10 mM β-CD clearly has an effect on the caveolae, which were significantly reduced in number and eventually disappeared almost completely from the plasma membrane.

Cholesterol depletion of CHO-EphB1 cells by β-CD, which leads to the loss of caveolae structures, did not affect the EphB1 receptor interaction with caveolin-1. Similar results were observed with 3T3-L1 adipocytes, in which the caveolin interaction with the insulin receptor was not altered by cholesterol depletion (Parpal et al., 2001). By contrast, in vascular smooth muscle cells, β-CD inhibited the autophosphorylation of EGF-R induced by angiotensin II, whereas the EGF-dependent EGF-R phosphorylation was not affected (Ushio-Fukai et al., 2001). In addition, we observed a significant reduction of EphB1-induced phosphorylation of ERK upon cholesterol depletion. Although cholesterol depletion in Rat-1 cells caused a marked increase in the amount of activated ERK (Furuchi and Anderson, 1998), caveolae-disrupting agents in mesangial cells significantly reduced endothelin-1 activation of ERK1/2 (Hua et al., 2003). These seemingly contradictory reports suggest that caveolae and caveolin-1 exert different actions depending upon the cellular context, receptor type and stimuli. In the case of EphB1, it appears that EphB1 receptors remain associated with the caveolin clusters and hence with the underlying caveolar remains or rafts after cholesterol depletion, but that intact caveolar cholesterol is required for downstream signaling through the MAPK pathway.

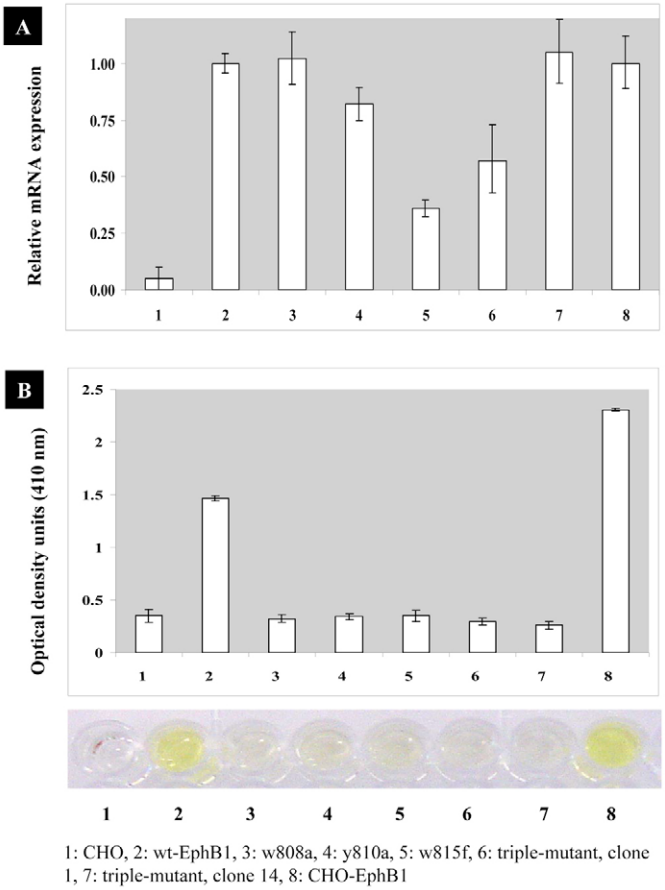

Fig. 4. Characterization of EphB1 mutants lacking the caveolin-binding motif. (A) Relative mRNA expression of EphB1 mutant and wild-type (wt) receptors was detected using real-time RT-PCR (numbers correspond to mutant and wt receptors listed at the bottom of the figure; for further details of the mutants, see text). The total RNA isolation was performed using Trizol® reagent. The 18S steady-state mRNA level was used as reference. The results showed that all of the EphB1 receptor constructs were expressed at the mRNA level. (B) ELISA was performed using the ephrinB2/Fc chimera to detect EphB1 expression on the cell membrane. The binding of the chimera was detected using AP-conjugated secondary antibody and color reaction was initiated by the addition of *p*-nitrophenyl phosphate. There was no detectable cell-surface expression of any of the mutant receptors when compared with CHO cells transfected with wild-type EphB1 receptor or with CHO-EphB1 cells. Results are representative of at least three independent experiments.

Fig. 5. EphB1 mutants lacking the caveolin-binding motif fail to localize to the cell membrane. The following were fixed and stained with anti-HA and anti-caveolin-1 primary antibodies followed by Alexa green- and red-conjugated secondary antibodies, respectively: CHO-EphB1 (O,P) and untransfected CHO cells (A,B); and CHO cells transiently transfected with wild-type EphB1 (C,D), mutant W808A (E,F), mutant Y810A (G,H), mutant W815F (I,J), triple mutant clone 1 (K,L), and triple mutant clone 14 (M,N). Samples were processed as described under Materials and Methods. The images are shown in two dimensions (A,C,E,G,I,K,M,O) and in three dimensions (B,D,F,H,J,L,N,P). Slides were viewed by laser-scanning confocal microscope with a ×63 objective. (Q) The percentage of EphB1 receptors localized on the membrane for each of the mutant EphB1 receptor constructs, as well as for non-transfected CHO cells (CHO), CHO cells transfected with wild-type receptor (wt-EphB1) and CHO-EphB1 cells, were calculated semi-quantitatively from representative cells and presented as % of the total number of the EphB1 receptors (n=3). (R-S) Examples of three-dimensional images (CHO-EphB1 cells and Y810A mutant, respectively) that were used for receptor counting and localization. The x, y and z axis are indicated in the images. Several cross-sections of each individual cell were used to localize the receptors in the three-dimensional images in Imaris 4.1.3. Software. Results are representative of at least three independent experiments.

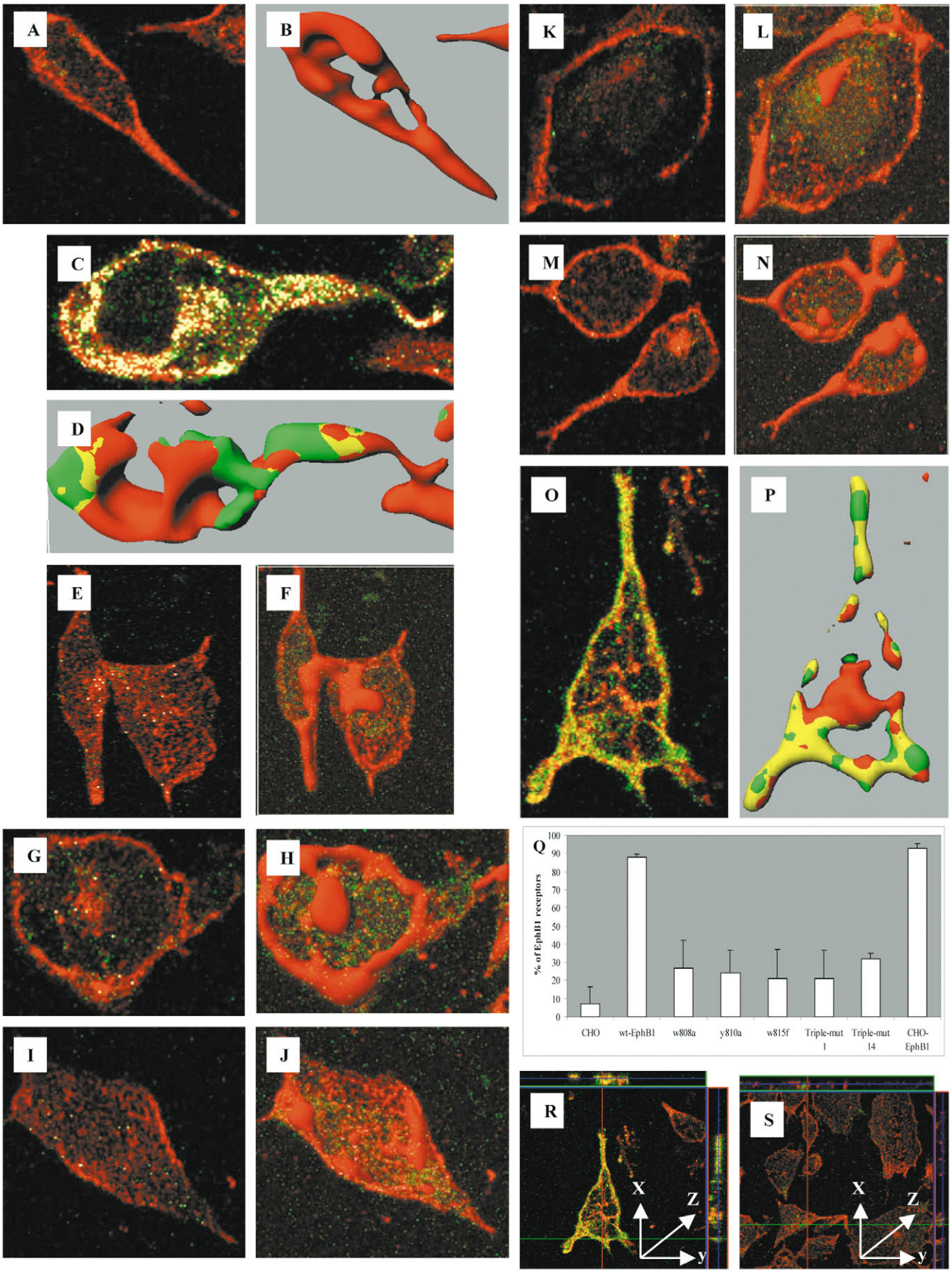

Fig. 5. See previous page for legend

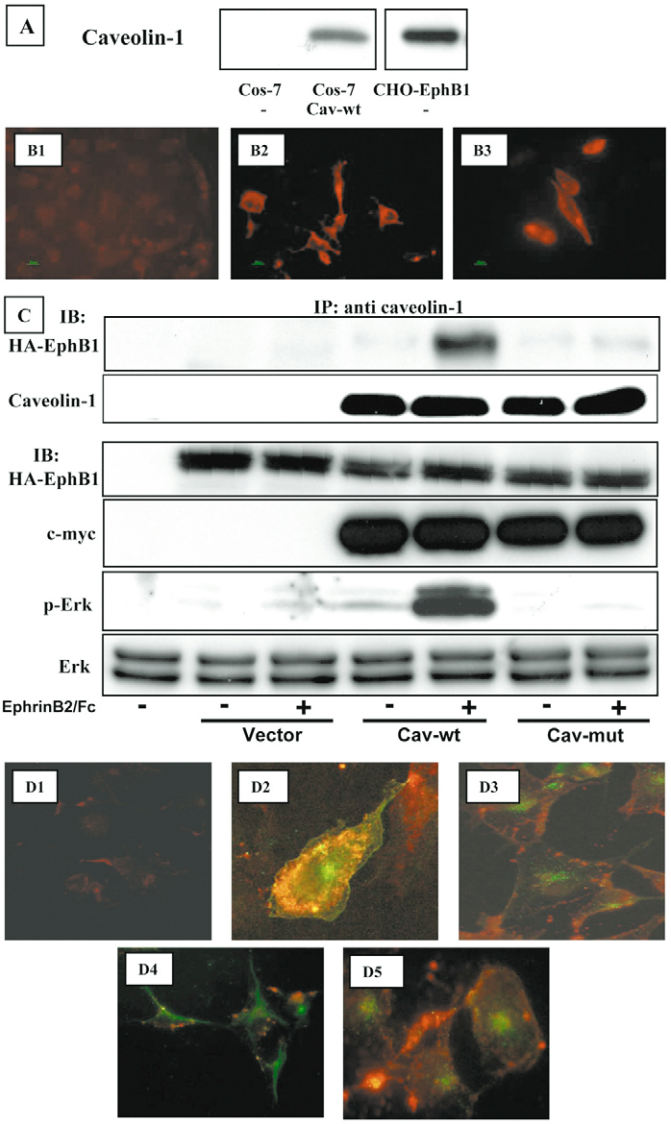

Fig. 6. The caveolin-1 scaffolding domain is required for interaction of EphB1 with caveolin-1 and for ERK activation by EphB1. (A,B) Expression of caveolin-1 in Cos-7 cells, Cos-7 cells transfected with wild-type caveolin-1 (Cav-wt), and CHO-EphB1 by immunoblotting (A) and by immunofluorescence (B1-B3, respectively). (B) The cells were fixed and stained with anti-caveolin-1 primary antibody followed by Alexa red-conjugated secondary antibody. Samples were processed as described under Materials and Methods. Images were acquired with a Nikon Eclipse E600 microscopy, connected to Nikon digital camera DXM1200, and processed with the Nikon AC-1 software version 2.11. Bars, 20 μm. (C) Cos-7 cells were transiently transfected with empty vector, wild-type (Cav-wt) or mutant caveolin-1 (Cav-mut) constructs, and additionally with wild-type EphB1 receptor: non-transfected Cos-7 cells (lane 1), empty vector (lanes 2-3), Cav-wt construct (lanes 4-5), and Cav-mut construct (lanes 6-7). Cells were co-transfected with wild-type EphB1 receptor (lanes 2-7). After 48 hours, the cells were incubated for 30 minutes with 1-2 μg/ml ephrinB2/Fc. Upper panel, co-immunoprecipitation of EphB1 receptor with anti-caveolin-1 antibody. The immunoprecipitates were resolved by SDS-PAGE and transferred to PVDF membranes. Membranes were probed with anti-HA or anti-caveolin-1, respectively. Lower panel, ephrinB2/Fc-induced ERK phosphorylation following transfection with the mentioned constructs was assessed using a phosphospecific antibody, then stripped blots were reprobed with anti-ERK antibody. (D) Cos-7 cells were transiently transfected with Cav-wt or Cav-mut constructs and additionally with wild-type or mutant EphB1 receptor: non-transfected Cos-7 cells (D1), Cos-7 cells transfected with wild-type EphB1 receptor and Cav-wt (D2), mutant EphB1 receptor and Cav-wt (D3), wild-type EphB1 receptor and Cav-mut (D4), and mutant EphB1 receptor and Cav-mut (D5). The cells were fixed and stained with anti-HA and anti-caveolin-1 primary antibodies followed by Alexa green- and red-conjugated secondary antibodies, respectively. Samples were processed as described under Materials and Methods. Images were acquired with a Nikon Eclipse E600 microscopy, connected to Nikon digital camera DXM1200, and processed with the Nikon AC-1 software version 2.11. Magnification, ×1000. Results are representative of at least three independent experiments.

As a complementary approach to studying the interaction between the EphB1 receptor and caveolin-1, we generated several EphB1 receptor mutants with a disrupted caveolin-binding motif. Our results showed that mutant EphB1 receptors were poorly expressed on the cell surface and instead were mainly found in the cytoplasm. Next, we used Cos-7 cells lacking endogenous caveolin-1 (Nystrom et al., 1999) (Fig. 6A,B) to determine the effect of reconstituted expression of wild-type caveolin-1 compared with mutant caveolin-1. The F92A and V94A mutations introduced into the Cav-mut construct disrupted the scaffolding domain of caveolin-1 (Nystrom et al., 1999). In Cos-7 cells, the Cav-mut construct completely lost its ability to co-immunoprecipitate with the EphB1 receptor after ligand stimulation, therefore suggesting that interactions between EphB1 and caveolin-1 depend on the caveolin-1 scaffolding domain. These results were confirmed with immunofluorescence analysis, in which we transiently transfected Cos-7 cells with Cav-wt or Cav-mut constructs and additionally with wild-type or mutant EphB1 receptor, and showed that only wild-type EphB1 receptor co-localized with Cav-wt, even if the Cav-mut also localized to the plasma membrane. Thus, the region of the EphB1 receptor containing the caveolin-1-binding motif is required for its correct membrane targeting. These results are reminiscent of the biological effect of a S522A mutation of the estrogen receptor, which resulted in decreased membrane receptor number, and reduced co-localization with caveolin and signaling to ERK (Razandi et al., 2003).

The Cav-mut construct completely abolished the phosphorylation of ERK/MAPK in response to ephrinB2 stimulation. To date, caveolin-1 has been shown to regulate negatively the activation state of the p42/44 MAPK cascade and other signaling pathways in many settings (Galbiati et al., 1998). However, our results are reminiscent of the effect of the caveolin mutant on the insulin receptor as shown by Nystrom and others (Nystrom et al., 1999). Moreover, a very recent study showed that, in Cav-1-transgenic mice, VEGF-induced ERK phosphorylation was markedly enhanced (Bauer et al., 2005).

To date, it has been shown that ephrins of both A and B subclasses can be found in lipid rafts. Moreover, there are indications that the ephrin-mediated ‘reverse signaling’ events are initiated within these micro-domains (Gauthier and Robbins, 2003). Our study now provides the first evidence that caveolae domains and their resident protein caveolin-1 also

play an important role in the regulation of EphB1 receptor expression and activity. Moreover, our demonstration of a stimulation-dependent association between caveolin and an A-subclass receptor (EphA2 in PC-3 cells) strongly suggests a global significance of this interaction. Our findings thus pave the way to define further the molecular mechanisms regulating the interaction between Ephs and ephrins and, ultimately, Eph-dependent angiogenesis.

Materials and Methods

Reagents and antibodies

Cell culture reagents were obtained from Invitrogen AG, ephrinB2/Fc and ephrinA1/Fc (ephrin/Fc consisting of the extracellular part of ephrin B2 or ephrin A1 fused to the Fc region of human immunoglobulin, respectively) from Amgen, control human IgG1 from Sigma, control rabbit IgG from Santa Cruz Biotechnology, and suramin was from Calbiochem (Merck Biosciences). The following antibodies were used for immunoprecipitation, immunoblotting or immunofluorescence: anti-caveolin-1 and anti-EphA2 (Santa Cruz Biotechnology), monoclonal anti-hemagglutinin (HA) (12CA5; Roche Diagnostics AG), monoclonal anti-caveolin-1 and anti-phospho-caveolin (Y14) (BD Transduction Laboratories), monoclonal anti-c-Myc (9E10) and anti-HA (Ha7) (Sigma), polyclonal rabbit anti-active-mitogen-activated protein kinase (MAPK; Promega), and polyclonal rabbit anti-extracellular-signal-regulated kinase (ERK1/2; Upstate Biotechnology). Bound antibodies were visualized using horseradish peroxidase (HRP)-conjugated goat anti-mouse or anti-rabbit secondary antibodies (Santa Cruz Biotechnology). ECL chemoluminescence kit was obtained from Amersham. The following antibodies were used for ELISA and confocal microscopy analysis: alkaline phosphatase (AP)-conjugated goat anti-human IgG (Jackson Immunoresearch Laboratories), and Alexa Fluor 495 goat anti-rabbit IgG and anti-mouse IgG, and Alexa Fluor 488 goat anti-mouse IgG (Molecular Probes).

Site-directed mutagenesis

Site-directed mutagenesis was performed using the overlap PCR technique. PCRs were performed using KlenTaq LA DNA polymerase (Sigma) with pSRα-hEphB1-HA plasmid as a template, which has been previously described (Stein et al., 1998). The oligonucleotides used to generate single or triple point mutations in the caveolin-1-binding motif in the human EphB1 receptor sequence were as follows (underlined nucleotides indicate the mutations): (A) W808A mutation: 1. round: 5′-ACC TGT CGG ACC GGT TAT T-3′ (sense) and 5′-ATA GCT TGC AAC GTC GCT GGC TGA A-3′ (antisense), and 5′-GAC GTT GCA AGC TAT GGG ATT CAC ATG TG-3′ (sense) and 5′-CTC ATG CCA TTG CCG TTG GT-3′ (antisense); (B) Y810A mutation: 1. round: 5′-ACC TGT CGG ACC GGT TAT T-3′ (sense) and 5′-TCC CAG CGC TCC AAA CGT CGC TGG-3′ (antisense), and 5′-GGA GCG CTG GGA TTC ACA TGT GGG AA-3′ (sense) and 5′-CTC ATG CCA TTG CCG TTG GT-3′ (antisense); (C) W815F mutation: 1. round: 5′-ACC TGT CGG ACC GGT TAT T-3′ (sense) and 5′-GAC TTC GAA CAT GTG AAT CCC ATA GCT C-3′ (antisense), and 5′-CAT GTT CGA AGT CAT GTA CTT TGG AGA-3′ (sense) and 5′-CTC ATG CCA TTG CCG TTG GT-3′ (antisense); 2. round: 5′-ACC TGT CGG ACC GGT TAT T-3′ (sense) and 5′-CTC ATG CCA TTG CCG TTG GT-3′ (antisense); (D) Triple mutation: 1. round: 5′-ACC TGT CGG ACC GGT TAT T-3′ (sense) and 5′-AAT CCC AGC GCT TGC AAC GTC-3′ (antisense), and 5′-GAC GTT GCA AGC GCT GGG ATT-3′ (sense) and 5′-CAT TGC CGT TGG TGA CTG A-3′ (antisense); 2. round: 5′-ACC TGT CGG ACC GGT TAT T-3′ (sense) and 5′-CAT TGC CGT TGG TGA CTG A-3′ (antisense). The triple mutation was created using the W815F-mutation-containing plasmid as a template, and mutating the other two proximal aromatic residues. Mutations were confirmed by nucleotide sequencing analysis (Microsynth AG).

Cell culture and transfection

Chinese hamster ovary (CHO)-EphB1 cells stably expressing HA-tagged EphB1 receptor have been described previously (Vindis et al., 2003) and were cultured in Dulbecco's Modified Eagle Medium-F12 (DMEM-F12) with 10% fetal calf serum (FCS) containing Zeocin (Invitrogen AG). CHO and African monkey kidney (Cos-7) cells were cultured in the same medium without Zeocin. Human prostate carcinoma (PC-3) cells were cultured in Dulbecco's Modified Eagle Medium with 10% FCS. For transient transfections, cells were seeded onto 100 mm plates or 6-well plates and incubated in culture medium for 24 hours before transfection. Cells were transfected using LipoFECTAMINE™ reagent (Invitrogen AG) with 4 or 1 μg of the plasmids encoding empty vector, wild-type or mutant caveolin-1 (kind gifts from M. Quon, NIH, Bethesda, MD), or wild-type or mutant EphB1 receptor indicated above. Co-transfection of the plasmid enhanced green fluorescent protein (pEGFP) was used at 1 μg/100 mm plate as a marker of transfection efficiency (~70%). Cells were used for biochemical or functional assays 48 hours later.

Detergent-free purification of caveolin-enriched membrane fractions

Caveolin-enriched membrane fractions were prepared as described previously (Song et al., 1996a). CHO-EphB1 cells were washed two times in ice-cold phosphate-buffered saline (PBS) and scraped into 0.5 ml 500 mM sodium carbonate, pH 11.0, transferred to a plastic tube, and homogenized in two steps using a 0.9×40 needle and an ultrasound bath (five times for 2-3 minutes). The homogenate was then adjusted to 45% sucrose by the addition of 0.5 ml 90% sucrose prepared in MBS (25 mM Mes, pH 6.5, 0.15 M NaCl) and placed at the bottom of an ultracentrifuge tube. A 5-35% discontinuous sucrose gradient was formed above (0.6 ml 5% sucrose, 2.4 ml 35% sucrose, both in MBS containing 250 mM sodium carbonate) and centrifuged at 38,000 rpm for 16-20 hours in an SW41 rotor (Beckman Instruments). Twelve 1 ml fractions were collected and analyzed by SDS-PAGE.

Quantitative real-time RT-PCR

Total RNA was isolated from CHO and CHO-EphB1 cells with Trizol® reagent (Invitrogen AG) according to the manufacturer's standard method. The total RNA was subjected to DNase treatment using DNaseI (Sigma) to degrade genomic DNA. The reverse transcription of the RNA pools was performed using Murine Leukemia Virus reverse transcriptase (MuLV) (Applied Biosystems) in GeneAmp PCR System 9700 (Applied Biosystems). Real-time RT-PCR was then performed using ABI Prism 7000 Sequence Detection System (Applied Biosystems). The Assays-on-Demand product purchased from Applied Biosystems contained Taqman minor groove binder (MGB) probe (6-FAM dye-labeled) combined with the primers for EphB1 receptor (Hs00174725_m1), and an Assays-on-Demand product for eukaryotic 18S ribosomal RNA (Hs99999901_s1) was used as endogenous control. The PCR was performed according to a previously described protocol (Nawrocki et al., 2002). The data were analyzed with ABI Prism 7000 SDS Software Version 1.1 (Applied Biosystems), and normalized to the expression level of eukaryotic 18S ribosomal RNA.

Immunoprecipitation and western blotting

CHO, CHO-EphB1, Cos-7 and PC-3 cells were serum starved for 24 hours in Opti-MEM (Invitrogen AG) and then treated with 0.5 mM suramin for 3 hours. Cells were then rinsed twice with PBS and incubated in 1% bovine serum albumin (BSA) for 45-60 minutes before stimulation for the indicated times at 37°C with 1-2 μg/ml of ephrinB2/Fc, ephrinA1/Fc or control IgG1. Cells were lysed in RIPA buffer for western blot analysis or in modified RIPA buffer for co-immunoprecipitation (Vindis et al., 2003), and 30 or 40 μg of protein was loaded on a 8 or 10% SDS-PAGE. After transfer to immobilon/polyvinylidene fluoride (PVDF) membranes (Millipore), proteins were detected with antibodies mentioned above. Membranes were then stripped and reprobed with appropriate antibodies to ensure equal loading of proteins. Immunoprecipitations were performed with the indicated antibodies overnight at 4°C as described previously (Vindis et al., 2004).

Electron microscopy analysis

For transmission electron microscopic studies, CHO-EphB1 cells treated with or without 10 mM β-cyclodextrin (β-CD) were fixed using a solution of 2.5% glutaraldehyde in 0.1 M cacodylate buffer (pH 7.4, 350 mOsm). Cells were centrifuged at 280 ***g*** for 1 minute. Cell pellets were post-fixed in osmium tetroxide, block-stained using uranyl acetate, dehydrated through ascending concentrations of ethanol and embedded in epoxy resin. Ultra-thin sections were obtained at 90 nm, counterstained with lead citrate and viewed on a Philips EM-300 microscope. For the scanning electron microscopy, the cells were fixed in the same fixative as above. Selected specimens were dehydrated through ascending concentrations of ethanol, critical point-dried in liquid carbon dioxide and mounted on aluminium stubs. The specimens were sputter-coated with gold and viewed under a Philips XL 30 FEG scanning electron microscope.

ELISA

We used 24-well plates (BD Biosciences) to perform ELISA. The cells were plated 12 hours before the experiments, and were fixed in 4% paraformaldehyde (PFA) for 10 minutes at 4°C. Plates were saturated for 1 hour at room temperature with PBS containing 10% fetal bovine serum (FBS). EphrinB2/Fc chimera (2 μg/ml) in PBS containing 10% FBS were then added to the wells. After overnight incubation at 4°C, the cells were washed (three times) with PBS. Binding of the chimera was detected using AP-conjugated goat anti-human IgG. The color reaction was initiated by the addition of *p*-nitrophenyl phosphate (Sigma). Optical density was measured on a micro plate reader at 410 nm.

Confocal microscopy analysis

CHO and CHO-EphB1 cells were plated on coverslips in 6-well dishes and cultured to 70% confluency. The cells were fixed in 4% PFA for 15 minutes on ice. Then the cells were permeabilized with 0.2% Triton X-100 in PBS for 15 minutes in room temperature, and saturated for 30 minutes at room temperature with PBS containing 1% BSA and 5% normal goat serum. Anti-HA and anti-caveolin-1 antibodies in blocking solution were then added on the cells. After overnight incubation at 4°C, the cells were washed (three times) with PBS. Binding of the primary antibodies

was detected using Alexa Fluor 488 goat anti-mouse IgG and Alexa Fluor 495 goat anti-rabbit IgG (Molecular Probes) secondary antibodies. Cells were then washed extensively (10-15 minutes) with PBS at room temperature and mounted in Vectashield (Vector Laboratories). Wide-field images were acquired using a Zeiss LSM 410 confocal microscope (Jena). Images were then processed using the LSM Image Browser software (Carl Zeiss AG), Huygens Essential deconvolution software (Scientific Volume Imaging BV), Imaris 4.1.3. (Bitplane AG) and Adobe Photoshop 5.5. The localization of the wild-type and mutant receptors were calculated semi-quantitatively from representative cells (n=3). Several cross-sections of each individual cell were used to localize the receptors in the three-dimensional images in Imaris 4.1.3. software as shown in Fig. 5R,S.

Statistical analysis

All values are presented as mean ± s.d. Analysis of variance (ANOVA) t test was used for statistical analysis, and differences were considered significant when P<0.05. Unless indicated otherwise, data are from at least three independent experiments.

References

Bauer, P. M., Yu, J., Chen, Y., Hickey, R., Bernatchez, P. N., Looft-Wilson, R., Huang, Y., Giordano, F., Stan, R. V. and Sessa, W. C. (2005). Endothelial-specific expression of caveolin-1 impairs microvascular permeability and angiogenesis. *Proc. Natl. Acad. Sci. USA* **102**, 204-209.

Brantley, D. M., Cheng, N., Thompson, E. J., Lin, Q., Brekken, R. A., Thorpe, P. E., Muraoka, R. S., Cerretti, D. P., Pozzi, A., Jackson, D. et al. (2002). Soluble Eph A receptors inhibit tumor angiogenesis and progression in vivo. *Oncogene* **21**, 7011-7026.

Brown, D. A. and London, E. (1998). Functions of lipid rafts in biological membranes. *Annu. Rev. Cell Dev. Biol.* **14**, 111-136.

Chang, W. J., Rothberg, K. G., Kamen, B. A. and Anderson, R. G. (1992). Lowering the cholesterol content of MA104 cells inhibits receptor-mediated transport of folate. *J. Cell Biol.* **118**, 63-69.

Christian, A. E., Haynes, M. P., Phillips, M. C. and Rothblat, G. H. (1997). Use of cyclodextrins for manipulating cellular cholesterol content. *J. Lipid Res.* **38**, 2264-2272.

Couet, J., Li, S., Okamoto, T., Ikezu, T. and Lisanti, M. P. (1997a). Identification of peptide and protein ligands for the caveolin-scaffolding domain. Implications for the interaction of caveolin with caveolae-associated proteins. *J. Biol. Chem.* **272**, 6525-6533.

Couet, J., Sargiacomo, M. and Lisanti, M. P. (1997b). Interaction of a receptor tyrosine kinase, EGF-R, with caveolins. Caveolin binding negatively regulates tyrosine and serine/threonine kinase activities. *J. Biol. Chem.* **272**, 30429-30438.

Dobrzanski, P., Hunter, K., Jones-Bolin, S., Chang, H., Robinson, C., Pritchard, S., Zhao, H. and Ruggeri, B. (2004). Antiangiogenic and antitumor efficacy of EphA2 receptor antagonist. *Cancer Res.* **64**, 910-919.

Drab, M., Verkade, P., Elger, M., Kasper, M., Lohn, M., Lauterbach, B., Menne, J., Lindschau, C., Mende, F., Luft, F. C. et al. (2001). Loss of caveolae, vascular dysfunction, and pulmonary defects in caveolin-1 gene-disrupted mice. *Science* **293**, 2449-2452.

Engelman, J. A., Chu, C., Lin, A., Jo, H., Ikezu, T., Okamoto, T., Kohtz, D. S. and Lisanti, M. P. (1998). Caveolin-mediated regulation of signaling along the p42/44 MAP kinase cascade in vivo. A role for the caveolin-scaffolding domain. *FEBS Lett.* **428**, 205-211.

Esser, S., Wolburg, K., Wolburg, H., Breier, G., Kurzchalia, T. and Risau, W. (1998). Vascular endothelial growth factor induces endothelial fenestrations in vitro. *J. Cell Biol.* **140**, 947-959.

Feron, O. and Kelly, R. A. (2001). The caveolar paradox: suppressing, inducing, and terminating eNOS signaling. *Circ. Res.* **88**, 129-131.

Fielding, P. E. and Fielding, C. J. (1995). Plasma membrane caveolae mediate the efflux of cellular free cholesterol. *Biochemistry* **34**, 14288-14292.

Folkman, J. (1995). Angiogenesis in cancer, vascular, rheumatoid and other disease. *Nat. Med.* **1**, 27-31.

Fujioka, K., Azuma, N., Kito, H., Gahtan, V., Esato, K. and Sumpio, B. E. (2000). Role of caveolin in hemodynamic force-mediated endothelial changes. *J. Surg. Res.* **92**, 7-10.

Furuchi, T. and Anderson, R. G. (1998). Cholesterol depletion of caveolae causes hyperactivation of extracellular signal-related kinase (ERK). *J. Biol. Chem.* **273**, 21099-21104.

Galbiati, F., Volonte, D., Engelman, J. A., Watanabe, G., Burk, R., Pestell, R. G. and Lisanti, M. P. (1998). Targeted downregulation of caveolin-1 is sufficient to drive cell transformation and hyperactivate the p42/44 MAP kinase cascade. *EMBO J.* **17**, 6633-6648.

Gale, N. W. and Yancopoulos, G. D. (1999). Growth factors acting via endothelial cell-specific receptor tyrosine kinases: VEGFs, angiopoietins, and ephrins in vascular development. *Genes Dev.* **13**, 1055-1066.

Garcia-Cardena, G., Fan, R., Stern, D. F., Liu, J. and Sessa, W. C. (1996). Endothelial nitric oxide synthase is regulated by tyrosine phosphorylation and interacts with caveolin-1. *J. Biol. Chem.* **271**, 27237-27240.

Gauthier, L. R. and Robbins, S. M. (2003). Ephrin signaling: one raft to rule them all? One raft to sort them? One raft to spred their call and in signaling bind them? *Life Sci.* **74**, 207-216.

Hua, H., Munk, S. and Whiteside, C. I. (2003). Endothelin-1 activates mesangial cell ERK1/2 via EGF-receptor transactivation and caveolin-1 interaction. *Am. J. Physiol. Renal Physiol.* **284**, F303-F312.

Kim, Y. N., Wiepz, G. J., Guadarrama, A. G. and Bertics, P. J. (2000). Epidermal growth factor-stimulated tyrosine phosphorylation of caveolin- 1. Enhanced caveolin-1 tyrosine phosphorylation following aberrant epidermal growth factor receptor status. *J. Biol. Chem.* **275**, 7481-7491.

Kimura, A., Mora, S., Shigematsu, S., Pessin, J. E. and Saltiel, A. R. (2002). The insulin receptor catalyzes the tyrosine phosphorylation of caveolin-1. *J. Biol. Chem.* **277**, 30153-30158.

Kullander, K. and Klein, R. (2002). Mechanisms and functions of Eph and ephrin signalling. *Nat. Rev. Mol. Cell Biol.* **3**, 475-486.

Kurzchalia, T. V. and Parton, R. G. (1999). Membrane microdomains and caveolae. *Curr. Opin. Cell Biol.* **11**, 424-431.

Labrecque, L., Royal, I., Surprenant, D. S., Patterson, C., Gingras, D. and Beliveau, R. (2003). Regulation of vascular endothelial growth factor receptor-2 activity by caveolin-1 and plasma membrane cholesterol. *Mol. Biol. Cell* **14**, 334-347.

Lee, H., Volonte, D., Galbiati, F., Iyengar, P., Lublin, D. M., Bregman, D. B., Wilson, M. T., Campos-Gonzalez, R., Bouzahzah, B., Pestell, R. G. et al. (2000). Constitutive and growth factor-regulated phosphorylation of caveolin-1 occurs at the same site (Tyr-14) in vivo: identification of a c-Src/Cav-1/Grb7 signaling cassette. *Mol. Endocrinol.* **14**, 1750-1775.

Li, S., Okamoto, T., Chun, M., Sargiacomo, M., Casanova, J. E., Hansen, S. H., Nishimoto, I. and Lisanti, M. P. (1995). Evidence for a regulated interaction between heterotrimeric G proteins and caveolin. *J. Biol. Chem.* **270**, 15693-15701.

Li, S., Seitz, R. and Lisanti, M. P. (1996a). Phosphorylation of caveolin by src tyrosine kinases. The alpha-isoform of caveolin is selectively phosphorylated by v-Src in vivo. *J. Biol. Chem.* **271**, 3863-3868.

Li, S., Song, K. S. and Lisanti, M. P. (1996b). Expression and characterization of recombinant caveolin. Purification by polyhistidine tagging and cholesterol-dependent incorporation into defined lipid membranes. *J. Biol. Chem.* **271**, 568-573.

Lisanti, M. P., Scherer, P. E., Vidugiriene, J., Tang, Z., Hermanowski-Vosatka, A., Tu, Y. H., Cook, R. F. and Sargiacomo, M. (1994). Characterization of caveolin-rich membrane domains isolated from an endothelial-rich source: implications for human disease. *J. Cell Biol.* **126**, 111-126.

Liu, P., Ying, Y., Ko, Y. G. and Anderson, R. G. W. (1996). Localization of platelet-derived growth factor-stimulated phosphorylation cascade to caveolae. *J. Biol. Chem.* **271**, 10299-10303.

Liu, J., Razani, B., Tang, S., Terman, B. I., Ware, J. A. and Lisanti, M. P. (1999). Angiogenesis activators and inhibitors differentially regulate caveolin-1 expression and caveolae formation in vascular endothelial cells. Angiogenesis inhibitors block vascular endothelial growth factor-induced down-regulation of caveolin-1. *J. Biol. Chem.* **274**, 15781-15785.

Mao, W., Luis, E., Ross, S., Silva, J., Tan, C., Crowley, C., Chui, C., Franz, G., Senter, P., Koeppen, H. et al. (2004). EphB2 as a therapeutic antibody drug target for the treatment of colorectal cancer. *Cancer Res.* **64**, 781-788.

Mastick, C. C. and Saltiel, A. R. (1997). Insulin-stimulated tyrosine phosphorylation of caveolin is specific for the differentiated adipocyte phenotype in 3T3-L1 cells. *J. Biol. Chem.* **272**, 20706-20714.

Mineo, C., James, G. L., Smart, E. J. and Anderson, R. G. (1996). Localization of epidermal growth factor-stimulated Ras/Raf-1 interaction to caveolae membrane. *J. Biol. Chem.* **271**, 11930-11935.

Nawrocki, A. R., Goldring, C. E., Kostadinova, R. M., Frey, F. J. and Frey, B. M. (2002). In vivo footprinting of the human 11beta-hydroxysteroid dehydrogenase type 2 promoter: evidence for cell-specific regulation by Sp1 and Sp3. *J. Biol. Chem.* **277**, 14647-14656.

Nystrom, F. H., Chen, H., Cong, L. N., Li, Y. and Quon, M. J. (1999). Caveolin-1 interacts with the insulin receptor and can differentially modulate insulin signaling in transfected Cos-7 cells and rat adipose cells. *Mol. Endocrinol.* **13**, 2013-2024.

Okamoto, T., Schlegel, A., Scherer, P. E. and Lisanti, M. P. (1998). Caveolins, a family of scaffolding proteins for organizing "preassembled signaling complexes" at the plasma membrane. *J. Biol. Chem.* **273**, 5419-5422.

Parpal, S., Karlsson, M., Thorn, H. and Stralfors, P. (2001). Cholesterol depletion disrupts caveolae and insulin receptor signaling for metabolic control via insulin receptor substrate-1, but not for mitogen-activated protein kinase control. *J. Biol. Chem.* **276**, 9670-9678.

Prinetti, A., Prioni, S., Chigorno, V., Karagogeos, D., Tettamanti, G. and Sonnino, S. (2001). Immunoseparation of sphingolipid-enriched membrane domains enriched in Src family protein tyrosine kinases and in the neuronal adhesion molecule TAG-1 by ganglioside monoclonal antibody. *J. Neurochem.* **78**, 1162-1167.

Razandi, M., Alton, G., Pedram, A., Ghonshani, S., Webb, P. and Levin, E. R. (2003). Identification of a structural determinant necessary for the localization and function of estrogen receptor alpha at the plasma membrane. *Mol. Cell. Biol.* **23**, 1633-1646.

Razani, B., Engelman, J. A., Wang, X. B., Schubert, W., Zhang, X. L., Marks, C. B., Macaluso, F., Russell, R. G., Li, M., Pestell, R. G. et al. (2001). Caveolin-1 null mice are viable but show evidence of hyperproliferative and vascular abnormalities. *J. Biol. Chem.* **276**, 38121-38138.

Razani, B., Woodman, S. E. and Lisanti, M. P. (2002). Caveolae: from cell biology to animal physiology. *Pharmacol. Rev.* **54**, 431-467.

Resh, M. D. and Erikson, R. L. (1985). Highly specific antibody to Rous sarcoma virus src gene product recognizes a novel population of pp60v-src and pp60c-src molecules. *J. Cell Biol.* **100**, 409-417.

Schnitzer, J. E., Oh, P., Pinney, E. and Allard, J. (1994). Filipin-sensitive caveolae-mediated transport in endothelium: reduced transcytosis, scavenger endocytosis, and capillary permeability of select macromolecules. *J. Cell Biol.* **127**, 1217-1232.

Schnitzer, J. E., Oh, P. and McIntosh, D. P. (1996). Role of GTP hydrolysis in fission of caveolae directly from plasma membranes. *Science* **274**, 239-242.

Shaul, P. W. and Anderson, R. G. (1998). Role of plasmalemmal caveolae in signal transduction. *Am. J. Physiol.* **275**, L843-L851.

Smart, E. J., Ying, Y., Donzell, W. C. and Anderson, R. G. (1996). A role for caveolin in transport of cholesterol from endoplasmic reticulum to plasma membrane. *J. Biol. Chem.* **271**, 29427-29435.

Song, K. S., Li, S., Okamoto, T., Quilliam, L. A., Sargiacomo, M. and Lisanti, M. P. (1996a). Co-purification and direct interaction of Ras with caveolin, an integral membrane protein of caveolae microdomains. *J. Biol. Chem.* **271**, 9690-9697.

Song, K. S., Scherer, P. E., Tang, Z., Okamoto, T., Li, S., Chafel, M., Chu, C., Kohtz, D. S. and Lisanti, M. P. (1996b). Expression of caveolin-3 in skeletal, cardiac, and smooth muscle cells. Caveolin-3 is a component of the sarcolemma and co-fractionates with dystrophin and dystrophin-associated glycoproteins. *J. Biol. Chem.* **271**, 15160-15165.

Stein, E., Huynh-Do, U., Lane, A. A., Cerretti, D. P. and Daniel, T. O. (1998). Nck recruitment to Eph receptor, EphB1/ELK, couples ligand activation to c-Jun kinase. *J. Biol. Chem.* **273**, 1303-1308.

Tanaka, T. and Kurth, R. (1984). Monoclonal antibodies specific for the avian sarcoma virus transforming protein pp60src. *Virology* **133**, 202-210.

Ushio-Fukai, M., Hilenski, L., Santanam, N., Becker, P. L., Ma, Y., Griendling, K. K. and Alexander, R. W. (2001). Cholesterol depletion inhibits epidermal growth factor receptor transactivation by Angiotensin II in vascular smooth muscle cells. Role of Cholesterol-rich microdomains and focal adhesions in Angiotensin II signaling. *J. Biol. Chem.* **276**, 48269-48275.

van Deurs, B., Roepstorff, K., Hommelgaard, A. M. and Sandvig, K. (2003). Caveolae: anchored, multifunctional platforms in the lipid ocean. *Trends Cell Biol.* **13**, 92-100.

Vihanto, M. M., Plock, J., Erni, D., Frey, B. M., Frey, F. J. and Huynh-Do, U. (2005). Hypoxia upregulates expression of Eph receptors and ephrins in mouse skin. *FASEB J.* **19**, 1689-1691.

Vindis, C., Cerretti, D. P., Daniel, T. O. and Huynh-Do, U. (2003). EphB1 recruits c-Src and p52Shc to activate MAPK/ERK and promote chemotaxis. *J. Cell Biol.* **162**, 661-671.

Vindis, C., Teli, T., Cerretti, D. P., Turner, C. E. and Huynh-Do, U. (2004). EphB1-mediated cell migration requires the phosphorylation of paxillin at Tyr-31/Tyr-118. *J. Biol. Chem.* **279**, 27965-27970.

Willingham, M. C., Jay, G. and Pastan, I. (1979). Localization of the ASV src gene product to the plasma membrane of transformed cells by electron microscopic immunocytochemistry. *Cell.* **18**, 125-134.

Yamamoto, M., Toya, Y., Schwencke, C., Lisanti, M. P., Myers, M. G., Jr and Ishikawa, Y. (1998). Caveolin is an activator of insulin receptor signaling. *J. Biol. Chem.* **273**, 26962-26968.

Yamamoto, M., Toya, Y., Jensen, R. A. and Ishikawa, Y. (1999). Caveolin is an inhibitor of platelet-derived growth factor receptor signaling. *Exp. Cell Res.* **247**, 380-388.

Yancey, P. G., Rodrigueza, W. V., Kilsdonk, E. P. C., Stoudt, G. W., Johnson, W. J., Phillips, M. C. and Rothblat, G. H. (1996). Cellular cholesterol efflux mediated by cyclodextrins. Demonstration of kinetic pools and mechanism of efflux. *J. Biol. Chem.* **271**, 16026-16034.

Zeidan, A., Broman, J., Hellstrand, P. and Swärd, K. (2003). Cholesterol dependence of vascular ERK1/2 activation and growth in response to stretch. *Arterioscler. Thromb. Vasc. Biol.* **23**, 1528-1534.

Journal of Cell Science